Comparison of Simplified Parametric Methods for Visual Interpretation of ^{11}C-Pittsburgh Compound-B PET Images

Marissa D. Zwan[1,2], Rik Ossenkoppele[1,2], Nelleke Tolboom[2], Alexandra J.M. Beunders[2], Reina W. Kloet[2], Sofie M. Adriaanse[1,2], Ronald Boellaard[2], Albert D. Windhorst[2], Pieter Raijmakers[2], Human Adams[2], Adriaan A. Lammertsma[2], Philip Scheltens[1], Wiesje M. van der Flier[1,3], and Bart N.M. van Berckel[2]

[1]Alzheimer Center and Department of Neurology, Neuroscience Campus Amsterdam, VU University Medical Center, Amsterdam, The Netherlands; [2]Department of Radiology and Nuclear Medicine, Neuroscience Campus Amsterdam, VU University Medical Center, Amsterdam, The Netherlands; and [3]Department of Epidemiology and Biostatistics, Neuroscience Campus Amsterdam, VU University Medical Center, Amsterdam, The Netherlands

This study compared several parametric imaging methods to determine the optimal approach for visual assessment of parametric Pittsburgh compound-B (^{11}C-PIB) PET images to detect cortical amyloid deposition in different memory clinic patient groups. **Methods:** Dynamic ^{11}C-PIB scanning of 120 memory clinic patients was performed. Parametric nondisplaceable binding potential (BP_{ND}) images were compared with standardized uptake value (SUV) and SUV ratio images. Images were visually assessed by 3 independent readers, and both interreader and intermethod agreement was determined. **Results:** Both 90-min (Fleiss κ = 0.88) and 60-min (Fleiss κ = 0.89) BP_{ND} images showed excellent interreader agreement, whereas agreement was good to moderate for SUV ratio images (Fleiss κ = 0.68) and SUV images (Fleiss κ = 0.59). Intermethod agreement varied substantially between readers, although BP_{ND} images consistently showed the best performance. **Conclusion:** The use of BP_{ND} images provided the highest interreader and intermethod agreement and is therefore the method of choice for optimal visual interpretation of ^{11}C-PIB PET scans.

Key Words: Alzheimer's disease; visual assessment; positron emission tomography; ^{11}C-PIB

Alzheimer disease (AD), the most common cause of dementia, is characterized by accumulation of the protein amyloid-β, which starts more than a decade before clinical symptoms occur (*1*). Recently, it has become possible to visualize and quantify this deposition in vivo using PET and the radiotracer Pittsburgh compound-B (^{11}C-PIB) (*2*). ^{11}C-PIB PET may be useful for distinguishing AD from other types of dementia, such as frontotemporal dementia and corticobasal degeneration (*3,4*). In patients with mild cognitive impairment (MCI), increased ^{11}C-PIB binding is predictive of conversion to AD (*5,6*). These findings underline the great potential of ^{11}C-PIB PET for early and accurate diagnosis of AD in different memory clinic patient groups.

In research applications, emphasis has been on quantitative or semiquantitative analysis of ^{11}C-PIB images. Receptor parametric mapping with fixed efflux rate constant (RPM2) has appeared to be more reliable quantitatively (*7*), although the main disadvantage of RPM2 compared with standardized uptake value ratio (SUVr) is a longer scan duration. For clinical purposes, visual interpretation of ^{11}C-PIB images may be sufficient rather than deriving quantitative measures. Previous studies have found a good correlation between visual interpretation of ^{11}C-PIB images and clinical diagnosis using either SUVr or RPM2 images (*8–10*). The aim of the present study was to compare the different parametric imaging methods to determine the optimal approach for visual assessment of ^{11}C-PIB images.

MATERIALS AND METHODS

Subjects

A total of 120 subjects with ^{11}C-PIB PET data available were included from the memory clinic–based Amsterdam Dementia Cohort. Clinical diagnosis was established without awareness of PET results and after a standard dementia screening (*11*). Thirty patients met the criteria of the National Institute on Aging–Alzheimer's Association for probable AD (*12*). Thirty patients were diagnosed as having non-AD dementia, including frontotemporal lobe dementia (*13*), Lewy body dementia (*14*), corticobasal degeneration (*15*), progressive supranuclear palsy (*16*), and vascular dementia (*17*). Thirty patients met the criteria of Petersen et al. (*18*) for MCI. The control group consisted of 30 subjects with subjective complaints or controls who had been recruited through advertisements in newspapers. Written informed consent was obtained from all patients. The Medical Ethics Review Committee of the VU University Medical Center approved this study.

PET

Dynamic PET scans were obtained using an ECAT EXACT HR+ scanner (Siemens/CTI) (*19*). The mean (±SD) injected activity was 369 ± 25 MBq and did not differ between groups ($P = 0.57$). Scanning was performed 4 ± 3 mo after the clinical diagnosis was made.

After ^{11}C-PIB injection, 4 different parametric ^{11}C-PIB images were generated: nondisplaceable binding potential (BP_{ND}) images using RPM2 applied to data from 0 to 60 min, BP_{ND} images using RPM2 applied to data from 0 to 90 min, SUV images of the 60- to 90-min interval (adjusted for injected mass and body weight), and SUVr images of the 60- to 90-min interval. For RPM2 and SUVr, cerebellar gray matter was used as reference tissue.

Three independent nuclear medicine physicians, masked to clinical information and MR imaging, assessed all images in a randomized order. The level of experience in visual reading of ^{11}C-PIB images

differed among readers. The most experienced reader rated multiple ^{11}C-PIB images each week, the second had substantial experience, and the third was a nuclear medicine physician in training.

Before definitive visual reading, a training session was conducted including mutual reading of 60 images, which had been generated by all 4 parametric methods based on data from 15 subjects not included in this study.

Transverse, sagittal, and coronal views were shown in the software package Vinci 2.56 (MPI für neurologische Forschung). Raters were able to scroll through the slices in the above-mentioned orientations and scale images manually using rainbow color scaling. Images were rated as either ^{11}C-PIB–positive (binding in more than one cortical brain region, that is, frontal, parietal, temporal, or occipital) or ^{11}C-PIB–negative (predominantly white matter binding).

Statistics

Differences between groups for baseline characteristics were assessed using ANOVA with post hoc Bonferroni, Kruskal–Wallis, and χ^2 tests, when appropriate. A P value of less than 0.05 was considered significant. Cohen κ for assessment of intermethod agreement between 2 methods and Fleiss κ for assessment of interreader agreement among 3 readers were calculated using SAS for Windows (Microsoft), version 9.2 (SAS Institute). Both were considered poor if κ was less than 0.20, satisfactory if κ was 0.21–0.40, moderate if κ was 0.41–0.60, good if κ was 0.61–0.80, and excellent if κ was more than 0.80.

RESULTS

The diagnostic groups did not significantly differ with respect to age (66 ± 8 y) or sex (33% female). As expected, controls scored higher on the Mini-Mental State Examination (score of 29) than MCI patients (score of 27, $P < 0.05$), who in turn scored higher than AD patients (score of 22, $P < 0.001$) and non-AD dementia patients (score of 24, $P < 0.05$). Furthermore, using 90-min BP_{ND} images, 93% of the AD patients were PIB-positive, followed by MCI patients (50%), healthy subjects (33%), and non-AD dementia patients (30%).

Interreader Agreement

Interreader agreement was excellent for visual assessment of 90-min BP_{ND} images (Fleiss $\kappa = 0.88$) and 60-min BP_{ND} images (Fleiss $\kappa = 0.89$), good for SUVr images (Fleiss $\kappa = 0.68$), and moderate for SUV images (Fleiss $\kappa = 0.59$; Table 1).

Between diagnostic groups, complete interreader agreement was found in the AD group (Fleiss $\kappa = 1.0$) for all analytic methods. For the other diagnostic groups, the highest agreement was found for both 60-min (Fleiss $\kappa = 0.82$–0.89) and 90-min BP_{ND} images (Fleiss $\kappa = 0.76$–0.91), followed by SUVr images (Fleiss $\kappa = 0.52$–0.73) and SUV images (Fleiss $\kappa = 0.44$–0.56) (Table 1).

TABLE 1
Interreader Agreement (Fleiss κ)

Parameter	SUV	SUVr	RPM2(90)	RPM2(60)
Overall	0.59	0.68	0.88	0.89
Healthy subjects	0.44	0.52	0.76	0.84
MCI	0.50	0.73	0.91	0.82
AD	1.0	1.0	1.0	1.0
Non-AD dementia	0.56	0.57	0.80	0.84

RPM2(90) and RPM2(60) indicate RPM2 applied on 90- and 60-min scans, respectively.

TABLE 2
Intermethod Agreement

Parameter	Reader A	Reader B	Reader C
Overall*	0.92	0.79	0.54
SUV–SUVr†	0.92	0.86	0.60
SUV–RPM2(90)†	0.93	0.80	0.51
SUVr–RPM2(90)†	0.95	0.83	0.52
SUV–RPM2(60)†	0.92	0.68	0.41
SUVr–RPM2(60)†	0.87	0.71	0.48
RPM2(90)–RPM2(60)†	0.88	0.83	0.74

*Expressed as Fleiss κ.
†Expressed as Cohen κ.
RPM2(90) and RPM2(60) indicate RPM2 applied on 90- and 60-min scans, respectively.

Intermethod Agreement

Intermethod agreement differed among readers, with moderate to good agreement (Fleiss $\kappa = 0.54$) between analytic methods seen in the reader with substantial experience and excellent agreement between analytic methods (Fleiss $\kappa = 0.92$) seen in the reader with most experience (Table 2). The least experienced reader showed intermediate results with good to excellent agreement (Fleiss $\kappa = 0.79$). Only for the comparison of 60-min and 90-min BP_{ND} images was intermethod agreement good to excellent (Cohen $\kappa = 0.74$–0.88) for all 3 readers.
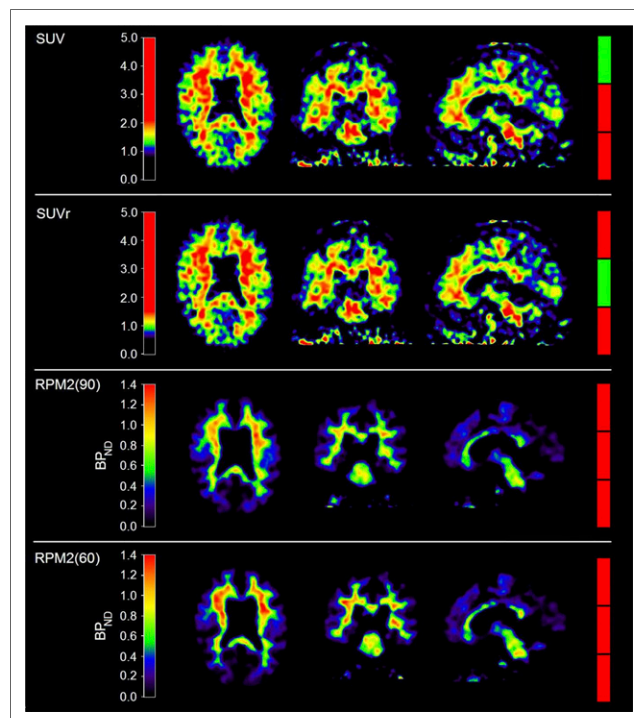

FIGURE 1. Example of visual interreader disagreement about different parametric ^{11}C-PIB images. From left to right are shown axial, coronal, and sagittal views. Colored bars on right indicate visual interpretation by 3 independent readers, with green indicating ^{11}C-PIB-positive rating and red ^{11}C-PIB-negative rating. RPM2(90) and RPM2(60) indicate RPM2 applied on 90- and 60-min scans, respectively.

Figure 1 shows an example of disagreement in visual rating of ^{11}C-PIB images of a frontotemporal dementia patient. Overall, the rating was ^{11}C-PIB–positive in 57% of the SUV images, 59% of the SUVr images, 51% of the 90-min BP_{ND} images, and 49% of the 60-min BP_{ND} images.

DISCUSSION

In the present study, excellent interreader agreement for visual interpretation of ^{11}C-PIB BP_{ND} images was found, with moderate to good agreement for SUVr and SUV images. Intermethod agreement varied substantially among readers, although both 60-min and 90-min BP_{ND} images consistently showed the best performance.

In accordance with previous studies, excellent interreader agreement for all investigated methods was found in the case of patients diagnosed with AD. In non-AD dementia patients, MCI patients, and controls, however, agreement among readers was poorer. A possible explanation is that amyloid deposition is a very early event and therefore a borderline amyloid load is seen mostly in the prodromal stages of AD. In addition, amyloid deposition can also be found in dementia with Lewy bodies, although this is generally lower and more variable than in AD (20). This variety in levels of amyloid deposition may lead to increased difficulty in visual reading, resulting in lower interreader agreement.

Substantial variation in reader performance was found with regard to intermethod agreement over the various methods, predominantly in the less experienced readers. Therefore, reading experience may have an impact on visual interpretation, and extensive training may be necessary to overcome the difficulty in reading SUV and SUVr images.

The best interreader agreement was found for BP_{ND} images. A disadvantage of the RPM2 method is the need for longer (dynamic) scans, which increase patient burden and the risk of patient motion. In the present study, 90- and 60-min BP_{ND} images showed comparable results regarding both interreader and intermethod agreement. Therefore, scan duration for BP_{ND} images used for visual interpretation may be limited to 60 min.

A major limitation of this study is the lack of a gold standard, as no postmortem data were available, hampering relating the findings to underlying neuropathology. Furthermore, because the time interval commonly used for generating SUVr images varies greatly, results cannot be generalized to SUVr images generated using other time intervals. We chose the 60- to 90-min interval because this is when pseudoequilibrium is nearly achieved (7).

These findings are important in light of new ^{18}F-labeled amyloid tracers that are expected to become widely available in the next few years to obtain SUVr images for clinical use. In addition, these tracers show lower target-to-background ratios than ^{11}C-PIB and higher white matter binding, which may increase reading difficulty. Therefore, caution is necessary for accurate reading of these newly available clinical tools.

CONCLUSION

BP_{ND} images showed the highest interreader and intermethod agreement in visual interpretation of ^{11}C-PIB images in the different memory clinic patient groups. It is therefore the method of choice for optimal visual interpretation of ^{11}C-PIB images. Reading experience may have an impact on visual interpretation, especially for SUVr and SUV images. Extensive training may be necessary to overcome the difficulty in reading SUV and SUVr images.

REFERENCES

1. Rowe CC, Ellis KA, Rimajova M, et al. Amyloid imaging results from the Australian Imaging, Biomarkers and Lifestyle (AIBL) study of aging. *Neurobiol Aging.* 2010;31:1275–1283.
2. Klunk WE, Engler H, Nordberg A, et al. Imaging brain amyloid in Alzheimer's disease with Pittsburgh Compound-B. *Ann Neurol.* 2004;55:306–319.
3. Rabinovici GD, Furst AJ, O'Neil JP, et al. ^{11}C-PIB PET imaging in Alzheimer disease and frontotemporal lobar degeneration. *Neurology.* 2007;68:1205–1212.
4. Ossenkoppele R, Prins ND, Pijnenburg YA, et al. Impact of molecular imaging on the diagnostic process in a memory clinic. *Alzheimers Dement.* 2013;9:414–421.
5. Okello A, Koivunen J, Edison P, et al. Conversion of amyloid positive and negative MCI to AD over 3 years: an ^{11}C-PIB PET study. *Neurology.* 2009;73:754–760.
6. Koivunen J, Scheinin N, Virta JR, et al. Amyloid PET imaging in patients with mild cognitive impairment: a 2-year follow-up study. *Neurology.* 2011;76:1085–1090.
7. Yaqub M, Tolboom N, Boellaard R, et al. Simplified parametric methods for [11C]PIB studies. *Neuroimage.* 2008;42:76–86.
8. Ng S, Villemagne VL, Berlangieri S, et al. Visual assessment versus quantitative assessment of ^{11}C-PIB PET and ^{18}F-FDG PET for detection of Alzheimer's disease. *J Nucl Med.* 2007;48:547–552.
9. Suotunen T, Hirvonen J, Immonen-Raiha P, et al. Visual assessment of [11C]PIB PET in patients with cognitive impairment. *Eur J Nucl Med Mol Imaging.* 2010;37:1141–1147.
10. Tolboom N, van der Flier WM, Boverhoff J, et al. Molecular imaging in the diagnosis of Alzheimer's disease: visual assessment of [11C]PIB and [18F] FDDNP PET images. *J Neurol Neurosurg Psychiatry.* 2010;81:882–884.
11. Tolboom N, Yaqub M, van der Flier WM, et al. Detection of Alzheimer pathology in vivo using both ^{11}C-PIB and ^{18}F-FDDNP PET. *J Nucl Med.* 2009;50:191–197.
12. McKhann GM, Knopman DS, Chertkow H, et al. The diagnosis of dementia due to Alzheimer's disease: recommendations from the National Institute on Aging-Alzheimer's Association workgroups on diagnostic guidelines for Alzheimer's disease. *Alzheimers Dement.* 2011;7:263–269.
13. Rascovsky K, Hodges JR, Knopman D, et al. Sensitivity of revised diagnostic criteria for the behavioural variant of frontotemporal dementia. *Brain.* 2011;134:2456–2477.
14. McKeith IG, Dickson DW, Lowe J, et al. Diagnosis and management of dementia with Lewy bodies: third report of the DLB Consortium. *Neurology.* 2005;65:1863–1872.
15. Boeve BF, Lang AE, Litvan I. Corticobasal degeneration and its relationship to progressive supranuclear palsy and frontotemporal dementia. *Ann Neurol.* 2003;54(suppl 5):S15–S19.
16. Litvan I, Agid Y, Calne D, et al. Clinical research criteria for the diagnosis of progressive supranuclear palsy (Steele-Richardson-Olszewski syndrome): report of the NINDS-SPSP international workshop. *Neurology.* 1996;47:1–9.
17. Román GC, Tatemichi TK, Erkinjuntti T, et al. Vascular dementia: diagnostic criteria for research studies—report of the NINDS-AIREN International Workshop. *Neurology.* 1993;43:250–260.
18. Petersen RC, Stevens JC, Ganguli M, Tangalos EG, Cummings JL, Dekosky ST. Practice parameter: early detection of dementia: mild cognitive impairment (an evidence-based review)—report of the Quality Standards Subcommittee of the American Academy of Neurology. *Neurology.* 2001;56:1133–1142.
19. Brix G, Zaers J, Adam LE, et al. Performance evaluation of a whole-body PET scanner using the NEMA protocol. *J Nucl Med.* 1997;38:1614–1623.
20. Rowe CC, Ng S, Ackermann U, et al. Imaging beta-amyloid burden in aging and dementia. *Neurology.* 2007;68:1718–1725.